ISSN 0036-0236, Russian Journal of Inorganic Chemistry, 2022, Vol. 67, No. 4, pp. 504–513. © Pleiades Publishing, Ltd., 2022.
ISSN 0036-0236, Russian Journal of Inorganic Chemistry, 2022. © Pleiades Publishing, Ltd., 2022.

PHYSICOCHEMICAL ANALYSIS OF INORGANIC SYSTEMS

Stable Phase Equilibria in the Quinary System Li^+, Na^+, K^+, Sr^{2+}//Br^-–H_2O at 308 K

X. F. Guo[a, b], S. H. Sang[a, b, *], and C. Ye[a, b]

[a] *College of Materials and Chemistry & Chemical Engineering, Chengdu University of Technology, Chengdu, 610059 China*

[b] *Mineral Resources Chemistry Key Laboratory of Sichuan Higher Education Institutions, Chengdu, 610059 China*

**e-mail: sangshihua@sina.com.cn*

Received August 6, 2021; revised November 12, 2021; accepted November 15, 2021

Abstract—The isothermal solution equilibrium method was used to study the phase equilibria of the quinary system LiBr–NaBr–KBr–$SrBr_2$–H_2O (saturated with KBr) at 308 K. Based on a large amount of experimental data, the phase equilibrium law of the quinary system was obtained. The experimental results indicated that the quinary system is a hydrate type, solid solution was not formed in the system, and the dry basis phase diagram (saturated with KBr) is composed of three invariant points, seven univariant curves and five saturated solid phase crystallization regions ($LiBr{\cdot}2H_2O$, NaBr, $NaBr{\cdot}2H_2O$, $SrBr_2{\cdot}2H_2O$, and $SrBr_2{\cdot}6H_2O$). Among these crystalline regions, $LiBr{\cdot}2H_2O$ has the smallest crystallization area and the largest solubility, which is difficult to separate from saturated solution. In the univariant curve with gradual addition of lithium bromide, the contents of potassium bromide, sodium bromide and strontium bromide all decrease gradually, while the contents of lithium bromide increase gradually, which indicates that lithium bromide has apparently salting out effect on potassium bromide, sodium bromide and strontium bromide. The equilibrium solid phase at three invariant points are identified by X-ray powder diffraction method as KBr + $LiBr{\cdot}2H_2O$ + $SrBr_2{\cdot}2H_2O$ + NaBr, KBr + NaBr + $SrBr_2{\cdot}2H_2O$ + $SrBr_2{\cdot}6H_2O$, and KBr + $NaBr{\cdot}2H_2O$ + NaBr + $SrBr_2{\cdot}6H_2O$.

Keywords: phase equilibrium, underground brine, solubility, bromide

DOI: 10.1134/S0036023622040076

INTRODUCTION

In recent years, the continuous emergence of problems such as illegal exploitation of solid mineral resources, low utilization rate and serious environmental damage has made the utilization of mineral resources not optimistic. The formation of mineral resources has experienced long-term development and evolution in the earth's crust. It is a natural mineral under certain geological conditions, and it is a nonrenewable resource with limited storage [1]. China is a country with a large population, and the per capita share of mineral resources is less than half of the world's per capita level. In view of the severe contradiction between supply and demand of solid mineral resources and China's basic national conditions that adhere to the path of sustainable development [2], the marine brine resources (such as sea water, salt lake brine, underground brine and other resources) with huge reserves, rich mineral elements content and high-grade value have become liquid mineral resources that can be utilized and developed by people, which can suspend the current serious shortage situation of domestic solid mineral resources [3]. However, the Sichuan Basin in China is a giant artesian basin rich in mineral resources. These mineral resources are of high grade and are widely distributed. They have a high degree of salinity. The total storage of underground brine is nearly 6 trillion cubic meters [4], which is rich in potassium, bromine, boron, lithium, strontium, etc. Therefore, the mineral resources in Sichuan Basin are of high exploitation value [5]. Among them, the average content of high-grade K^+ is 18.86 g/L, the average content of Br^- is 300 mg/L, and even can reach the highest content of 2533–2640 mg/L. The content of these elements reaches or exceeds the national mining and utilization indicators and they are a very valuable asset [6]. In order to carry out phase equilibrium experimental research on the lithium, potassium and strontium system in underground brine in the Sichuan Basin, it is necessary to fully understand the phase separation technology and the theory of the phase diagram of the water-salt system, and grasp the basic laws of brine salting out and mineralization, so as to guide production and process research more scientifically and effectively.

Regarding the phase equilibrium study of underground brine rich in multiple useful components in the Sichuan Basin, Zeng et al. have carried out a series of phase equilibrium studies on underground brine which is rich in potassium, rubidium, boron and other

Table 1. Experimental Reagents, Purity AR (mass fraction ≥ 99%)

Reagent name	CAS	Purification method	Source
Lithium bromide (LiBr)	7550-35-8	Chemical analysis	Shanghai Aladdin Biochemical Technology Co., Ltd.
Sodium bromide (NaBr)	7647-15-6	Chemical analysis	Chengdu Kelong Chemical Reagent Factory
Potassium bromide (KBr)	7758-02-3	Chemical analysis	Chengdu Kelong Chemical Reagent Factory
Strontium bromide	7789-53-9	Chemical analysis	Shanghai Aladdin Biochemical Technology Co., Ltd.

beneficial components in the Sichuan Basin. For instance, the study of the metastable phase equilibria in the aqueous ternary system at 298.15 K [7], solubility of the reciprocal quaternary system Li^+, $Na^+//CO_3^{2-}$, $SO_4^{2-}-H_2O$ at 273.15 K [8], solid–liquid equilibria in the aqueous system containing the chlorides of lithium, rubidium and magnesium at 323 K [9], and other stable or metastable phase equilibria of the relevant sub-systems of the system Li–K–Rb–Mg–Cl–B_4O_7–H_2O from 298.15 to 348.15 K [10–17]. And our research group is mainly to carry out multi-temperature phase equilibrium research on the underground brine rich in potassium, bromide, strontium and boron in the Sichuan Basin, and has completed the solubility study of two quaternary systems NaBr–Na_2SO_4–KBr–K_2SO_4–H_2O and KCl–KBr–$K_2B_4O_7$–H_2O at 323 K. In addition, the phase equilibria study of the ternary system KBr–$K_2B_4O_7$–H_2O at 298, 323 and 348 K [18–20], the quinary system Na^+, $K^+//Cl^-$, SO_4^{2-}, $B_4O_7^{2-}-H_2O$ at 298, 323 K [21–23], and the quinary system $K^+//Cl^-$, Br^-, SO_4^{2-}, $B_4O_7^{2-}-H_2O$ at 323, 348 K have been published [24–28].

In addition, researchers have also done a lot of experimental research on the system containing Br^- in the water-salt system. For instance, the ternary system KCl–KBr–H_2O at 298–373 K [29], the quaternary system KCl–KBr–$K_2B_4O_7$–H_2O at 323 and 373 K [30–33], and the quinary system KCl–KBr–K_2SO_4–$K_2B_4O_7$–H_2O stable phase equilibria at 323 and 348 K [34–38], It is found that the above systems are easy to form solid solution K(Cl, Br). At the same time, there are many theoretical calculations of water salt system containing bromine. Examples include ternary systems KBr–$K_2Cr_2O_7$–H_2O and KBr–C_SBr–H_2O solubility prediction at 298 K and theoretical calculation of phase equilibrium of the interactive quaternary system NaBr–KBr–Na_2SO_4–K_2SO_4–H_2O at 323 K. And Hu et al. completed the quaternary system NaBr–KBr–$MgBr_2$–H_2O, NaBr–KBr–$CaBr_2$–H_2O and ternary system NaBr–$MgBr_2$–H_2O, KBr–$MgBr_2$–H_2O, NaBr–$CaBr_2$–H_2O, KBr–$CaBr_2$–H_2O and $CaBr_2$–$MgBr_2$–H_2O at 348 K experimental study and theoretical calculation of phase equilibrium [39–41]. From the above studies, it can be seen that scholars have few studies on the bromine-containing quinary system, so it is of great significance to carry out the research on the enrichment of bromine-containing system by carrying out LiBr–NaBr–KBr–$SrBr_2$–H_2O.

The study of the phase equilibria of the water-salt system is helpful to promote the development and utilization of salt lake resources. Therefore, the work will focus on the study of the stable phase equilibria of the quinary system Li^+, Na^+, K^+, $Sr^{2+}//Br^-$–H_2O under the complex multi-component system in the underground brine of the Sichuan Basin at 308 K, which is not only a supplement to the study of the phase equilibria of the water-salt system, but also provides a scientific guidance for the rational development and utilization of the precious resources of the underground brine, especially for the improvement and promotion of the extraction of sodium, lithium, potassium, strontium.

EXPERIMENTAL

Reagents and instruments. During preparing the solid–liquid mixed material and liquid samples of each system, the chemical reagents involved, the names and purity of the reagents used in the chemical analysis process and the manufacturers are listed in Table 1. And the water used in the whole experiment is deionized water made by the instrument in the laboratory, its pH is about 6.6, and its conductivity is less than 1.2×10^{-5} S m^{-1}. The deionized water should be boiled to remove CO_2 when used in experiments. All reagents have reached analytical purity.

The main instruments and equipment used in the experimental research are listed in Table 2. In addition, some conventional glass instruments are also used. For example, in process of preparing solid-liquid mixture samples of the quinary systems, 50 mL frosted glass bottles are used, as well as volumetric flasks, conical flasks, burettes, beakers, pipettes and other glass instruments used in chemical analysis.

Experimental methods. The research object of this article is phase equilibrium law in the quinary system

Table 2. Experimental equipments and instruments

Instrument name	Type and accuracy	Manufacturing company
Atomicabsorption spectrometer	ICE 3300	American Thermo Scientific
Incubator	SHH-250 (precision: ±0.1 K)	Chongqing Yingbo Experimental Instrument Co., Ltd
Constant temperature water bath oscillator	HZS-H (precision: ±0.1 K)	Harbin Donglian Electronic Technology Co., Ltd.
Oscillator	HY-5	Jintan Kexi Instrument Co., Ltd.
Electronic balance	AL 104(precision: 0.0001 g)	The Mettler Toledo Instruments Co., Ltd.
Ultrapure water device	UPT-II-20T	Youpu Chaochun Technology Co., Ltd.
X-ray diffraction	DX-2700	Danfangyuan Instrument Co., Ltd.

Li^+, Na^+, K^+, $Sr^{2+}//Br^--H_2O$, which is a stable phase equilbrium system and studied by the mature isothermal solution equilibrium method. On the basis of consulting various inorganic salt solubility manuals and a large number of related system documents, the general trend of the solubility of each component is predicted.

The specific method is to add another inorganic salt to a certain ratio according to the data of the invariant point of the quaternary subsystems under a constant temperature condition, and then add a fixed amount of distilled water to the experimental bottle containing the mixed salt, later seal its mouth well. The prepared samples are placed in a circulating shaker, and then placed in a constant temperature biochemical incubator together with the shaker, and the temperature of the incubator is adjusted to 308 K (±0.1 K), so that the sample is sufficiently shaken under constant temperature conditions to accelerate the equilibrium. After a period of time, turn off the oscillator, wait for the sample in the experiment bottle to stand sufficiently to completely separate the solid and liquid phases, and then take the supernatant of the experiment bottle for quantitative analysis of the liquid phase content composition, and wait for the content composition of each substance to remain unchanged which will as a criterion for the system to reach equilibrium. After confirming that the system has reached equilibrium, we used a pipette to quantitatively take the supernatant into a volumetric flask, and then make a volumetric analysis of each substance's content and composition. At the same time, we need to take out a certain sedimentary solid phase. After suction filtration, washing, and sufficient grinding, solid phase identification was performed.

Analytical methods. The content of each ion in the equilibrium liquid phase is determined by chemical analysis. Potassium ion is titrated with sodium tetraphenylborate quaternary ammonium salt back titration method (STPB method) [42], and the uncertainty is 0.5%. The measurement of lithium ions adopts atomic absorption spectrophotometry (relative standard uncertainty of 0.5%). The amount of bromine ion was determined by a silver nitrate standard solution (relative standard uncertainty of 0.3%) with potassium dichromate as an indicator in nearly neutral solution, and the sodium ion content was determined by the ion balance subtraction method (relative standard uncertainty of 0.5%). The strontium ion is titrated by the ethylenediaminetetraacetic acid volumetric method (relative standard uncertainty of 0.5%) [43, 44]. The equilibrium solid phase is identified by the X-ray powder crystal diffraction method, and the X-ray powder crystal diffraction pattern of the solid samples is compared with the standard pattern to determine its equilibrium solid phase composition.

RESULTS AND DISCUSSION

Based on chemical analysis of the saturated liquid phase of the quinary system $LiBr-NaBr-KBr-SrBr_2-H_2O$ at 308 K, the solubility data of the equilibrium liquid phase are obtained and presented in Table 3, and the corresponding components of the Jänecke index J (Jänecke index) was also calculated.

Taking $J(NaBr) + J(LiBr) + J(SrBr_2) = 100$ g as the benchmark (saturated with KBr) and $J(SrBr_2)$ as the abscissa, the simplified dry basis diagram (Fig. 1a), the partially enlarged simplified dry basis diagram (Fig. 1b) and the corresponding water content change diagram (Fig. 2) of the quinary system are drawn with potassium bromide saturation as the projection plane. In order to understand the dissolution of potassium bromide in the solution, the variation of potassium bromide content with $J(SrBr_2)$ is also plotted in Fig. 3,

Table 3. Solubilities of salts in the quinary system LiBr–NaBr–KBr–$SrBr_2$–H_2O (saturated with KBr) at 308 K and pressure p = 0.1 MPa

No.	Liquid phase composition(100·w(b))				Dry salt composition J_b, g/100 g J(LiBr) + J(NaBr) + J($SrBr_2$) = 100 g					Equilibrium solids
	KBr	w(LiBr)	w(NaBr)	w($SrBr_2$)	J(KBr)	J(LiBr)	J(NaBr)	J($SrBr_2$)	J(H_2O)	
1, A	2.16	61.24	0.64	0.00	3.49	98.97	1.03	0.00	58.11	LH + N + K
2	2.17	61.73	0.60	0.71	3.44	97.92	0.95	1.12	55.19	LH + N + K
3	2.12	61.67	0.60	1.02	3.35	97.44	0.95	1.61	54.64	LH + N + K
4, B	4.80	24.54	22.58	0.00	10.18	52.08	47.92	0.00	102.06	N + NH + K
5	4.80	24.05	22.42	1.65	9.97	49.99	46.59	3.42	97.88	N + NH + K
6	4.71	23.82	21.37	3.14	9.74	49.29	44.22	6.50	97.17	N + NH + K
7	4.45	21.65	18.56	9.09	9.02	43.92	37.65	18.43	93.81	N + NH + K
8	4.28	21.41	16.54	12.21	8.53	42.69	32.97	24.34	90.85	N + NH + K
9	4.01	21.71	14.20	15.03	7.88	42.61	27.88	29.51	88.40	N + NH + K
10, C	2.18	60.64	0.00	1.45	3.51	97.66	0.00	2.34	57.55	LH + K + S
11, E_1	2.10	60.57	0.60	1.45	3.35	96.73	0.96	2.32	56.34	LH + K + S + N
12, D	2.04	51.62	0.00	6.85	3.48	88.28	0.00	11.72	67.55	K + S + SH
13	2.02	51.75	0.30	7.14	3.41	87.43	0.51	12.06	65.54	K + S + SH
14	2.00	51.54	0.58	7.22	3.36	86.84	0.98	12.17	65.13	K + S + SH
15, F	5.22	0.00	20.70	31.67	9.97	0.00	39.53	60.47	80.98	K + SH + NH
16	4.88	2.27	20.22	30.66	9.18	4.27	38.05	57.68	78.98	K + SH + NH
17	4.73	5.41	19.64	28.37	8.86	10.12	36.77	53.11	78.33	K + SH + NH
18	4.46	9.21	18.40	24.82	8.50	17.57	35.09	47.35	82.23	K + SH + NH
19	4.06	15.45	14.86	20.33	8.01	30.51	29.34	40.15	89.44	K + SH + NH
20, E_3	3.99	20.59	13.20	17.79	7.74	39.92	25.59	34.49	86.18	K + SH + NH + N
21	3.94	20.96	12.84	17.49	7.69	40.86	25.04	34.09	87.29	K + SH + N
22	3.61	25.87	10.53	14.60	7.08	50.73	20.64	28.63	89.00	K + SH + N
23	2.89	37.17	5.62	9.04	5.57	71.70	10.85	17.45	87.35	K + SH + N
24, E_2	2.00	51.18	1.00	7.18	3.37	86.21	1.69	12.10	65.09	K + SH + N + S
25	2.01	52.90	0.93	5.67	3.37	88.91	1.56	9.53	64.69	K + N + S
26	2.07	59.91	0.63	1.61	3.33	96.38	1.02	2.60	57.55	K + N + S

K: KBr, LH: LiBr·2H_2O, N: NaBr, NH: NaBr·2H_2O, S: $SrBr_2$·2H_2O, SH: $SrBr_2$·6H_2O; Relative standard uncertainty $u(T)$ = 0.5 K, $u(\rho)$ = 0.0002 g cm^{-3}; $u_r(w(NaBr)$ = 0.005, $u_r(w(KBr)$ = 0.005, $u_r(w(LiBr)$ = 0.005, $u_r(w(SrBr_2)$ = 0.005.

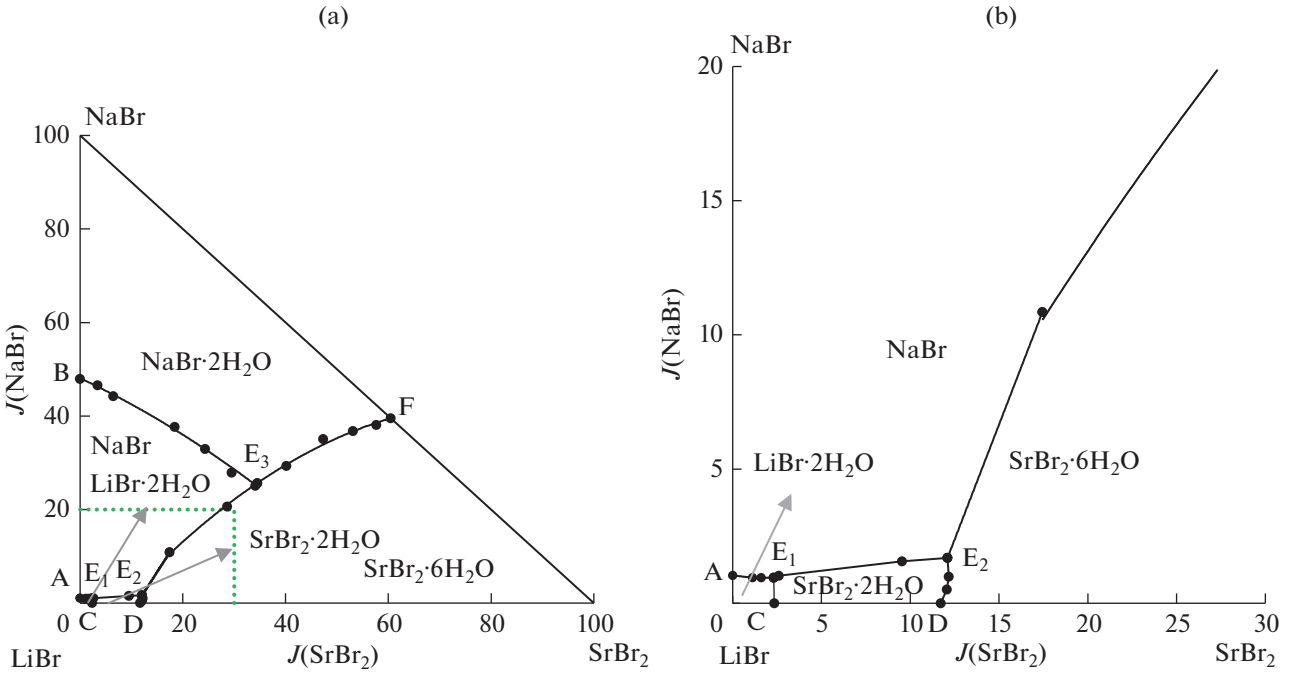

Fig. 1. (a) Simplified dry basis phase diagram of the quinary system LiBr–NaBr–KBr–$SrBr_2$–H_2O (saturated with KBr) at 308 K; (b) local enlarged simplified dry basis phase diagram of the quinary system LiBr–NaBr–KBr–$SrBr_2$–H_2O (saturated with KBr) at 308 K.

and the saturated solid phase at the invariant points are identified by X-ray diffraction experiments. The XRD patterns of equilibrium solid phase at these invariant points are given in Figs. 4–6.

From Table 3 and the dry basis phase diagram Fig. 1, it can be seen that the quinary system LiBr–NaBr–KBr–$SrBr_2$–H_2O is a hydrate type system, double salt and solid solution were not found. According to reported literature, $K_{1-x}Na_xBr$ solid solution can be prepared by melting a mixture of KBr and NaBr under

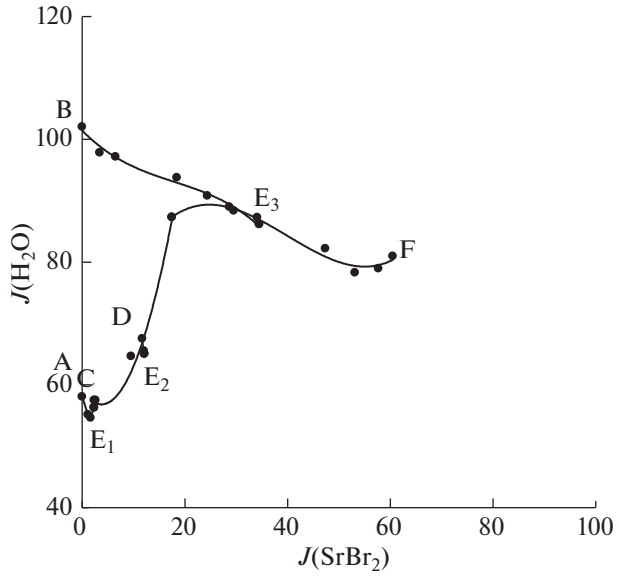

Fig. 2. Water content diagram of the quinary system LiBr–NaBr–KBr–$SrBr_2$–H_2O (saturated with KBr) at 308 K.

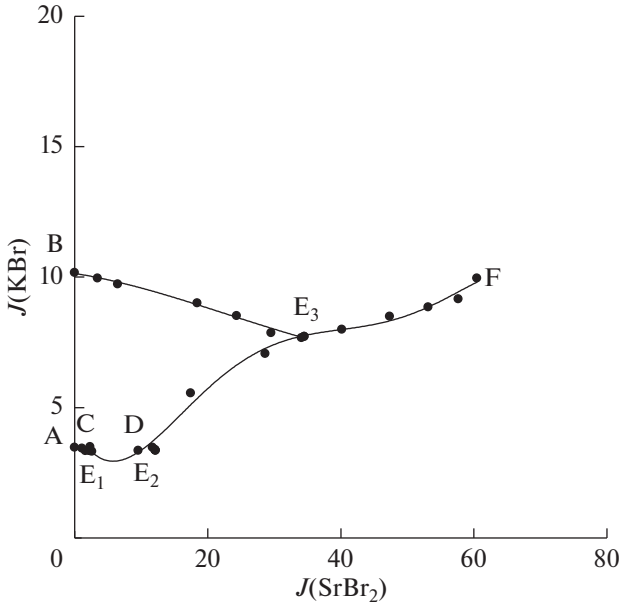

Fig. 3. Content diagram of potassium bromide in the quinary system LiBr–NaBr–KBr–$SrBr_2$–H_2O (saturated with KBr) at 308 K.

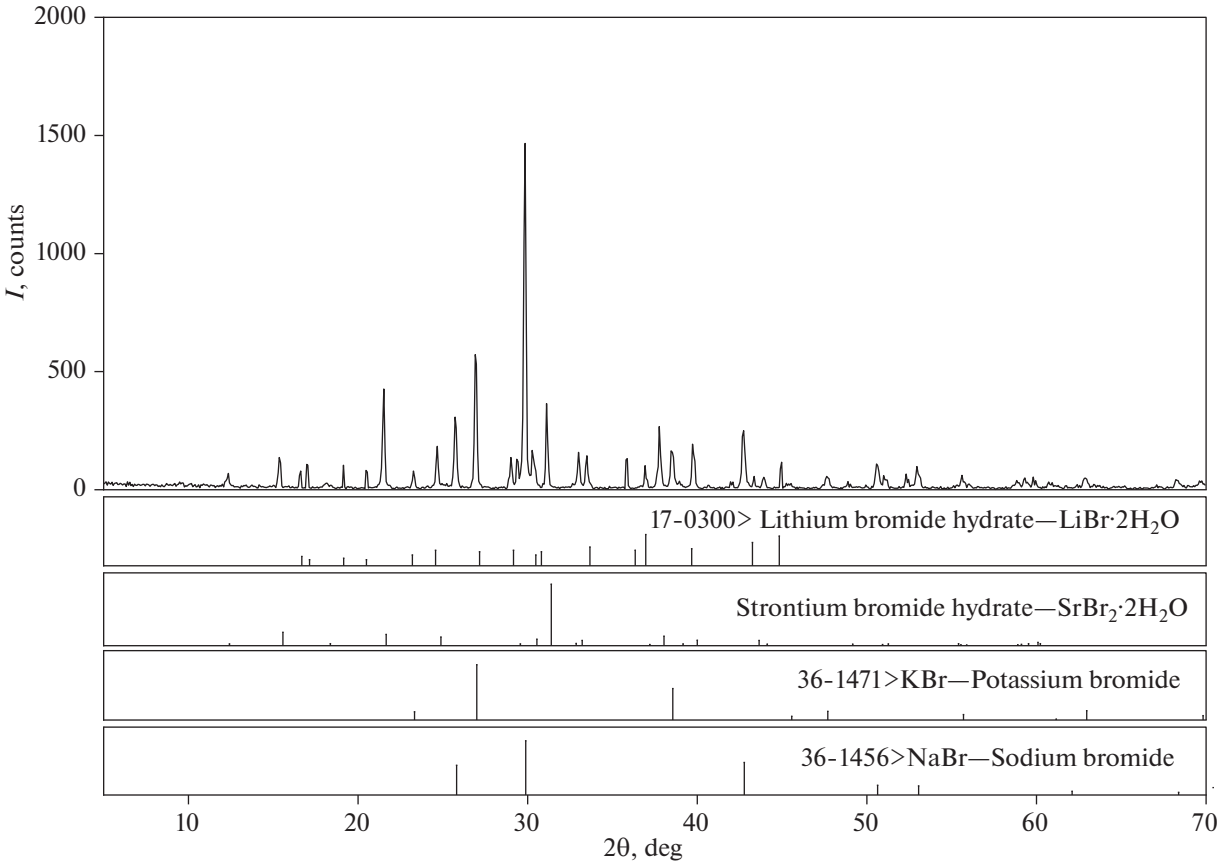

Fig. 4. X–ray powder diffraction photograph of equilibrium solid phases at invariant point E_1 (KBr + LiBr·$2H_2O$ + $SrBr_2$·$2H_2O$ + NaBr) in the quinary system LiBr–NaBr–KBr–$SrBr_2$–H_2O (saturated with KBr) at 308 K.

vacuum conditions higher than 200°C and then cooling to room temperature [44]. Combined with research experience of our research team in KBr–NaBr related water-salt system, it is also confirmed that no $K_{1-x}Na_xBr$ solid solution is formed in the quinary water-salt system Li^+, Na^+, K^+, Sr^{2+}//Br^-–H_2O at 308.15 K.

The dry basis phase diagram of the quinary system LiBr–NaBr–KBr–$SrBr_2$–H_2O is composed of three invariant points, seven univariant curves and five solid phase crystal regions, details as follows. The dry basis phase diagram of the quinary system LiBr–NaBr–KBr–$SrBr_2$–H_2O at 308 K contains five boundary points, these five boundary points are also the invariant points of the quaternary subsystems LiBr–NaBr–KBr–H_2O, LiBr–KBr–$SrBr_2$–H_2O, and NaBr–KBr–$SrBr_2$–H_2O, where points A and B are two invariant points of the quaternary system LiBr–NaBr–KBr–H_2O, the corresponding saturated solid phases are LiBr·$2H_2O$ + NaBr + KBr and NaBr + NaBr·$2H_2O$ + KBr respectively. Points C and D are the two invariant points of the quaternary system LiBr–KBr–$SrBr_2$–H_2O, and the corresponding saturated solid phases are LiBr·$2H_2O$ + KBr + $SrBr_2$·$2H_2O$ and $SrBr_2$·$6H_2O$ + $SrBr_2$·$2H_2O$ + KBr respectively. The quaternary system NaBr–KBr–$SrBr_2$–H_2O has only one invariant point F, and the corresponding equilibrium solid phase is NaBr·$2H_2O$ + $SrBr_2$·$6H_2O$ + KBr. Points E_1, E_2 and E_3 are the three invariant points of the quinary system LiBr–NaBr–KBr–$SrBr_2$–H_2O, the saturated equilibrium solid phase at E_1 point is KBr + LiBr·$2H_2O$ + $SrBr_2$·$2H_2O$ + NaBr, and the equilibrium liquid phase is expressed in mass fraction as w(KBr) = 2.10%, w(LiBr) = 60.57%, w(NaBr) = 0.60%, w($SrBr_2$) = 1.45%. The saturated equilibrium solid phase at E_2 point is KBr + NaBr + $SrBr_2$·$2H_2O$ + $SrBr_2$·$6H_2O$, and the equilibrium liquid phase is expressed in mass fraction as w(KBr) = 2.00%, w(LiBr) = 51.18%, w(NaBr) = 1.00%, w($SrBr_2$) = 7.18%. The saturated equilibrium solid phase at point E_3 is KBr + NaBr·$2H_2O$ + NaBr + $SrBr_2$·$6H_2O$, and the equilibrium liquid phase is expressed in mass fraction as w(KBr) = 3.99%, w(LiBr) = 20.59%, w(NaBr) = 13.20%, w($SrBr_2$) = 17.79%. The identifications of the equilibrium solid phases at the invariant points E_1, E_2 and

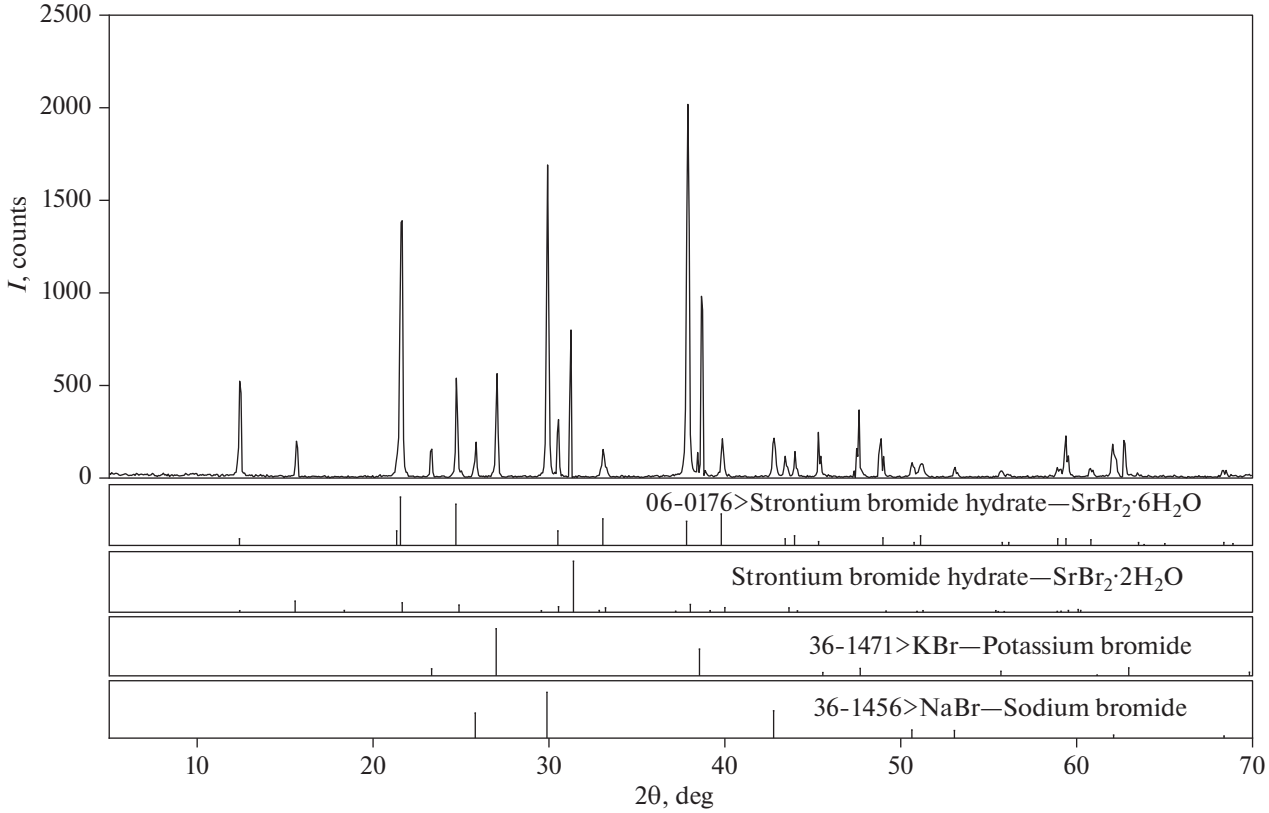

Fig. 5. X–ray powder diffraction photograph of equilibrium solid phases at invariant point E_2 (KBr + NaBr + $SrBr_2 \cdot 2H_2O$ + $SrBr_2 \cdot 6H_2O$) in the quinary system LiBr–NaBr–KBr–$SrBr_2$–H_2O (saturated with KBr) at 308 K.

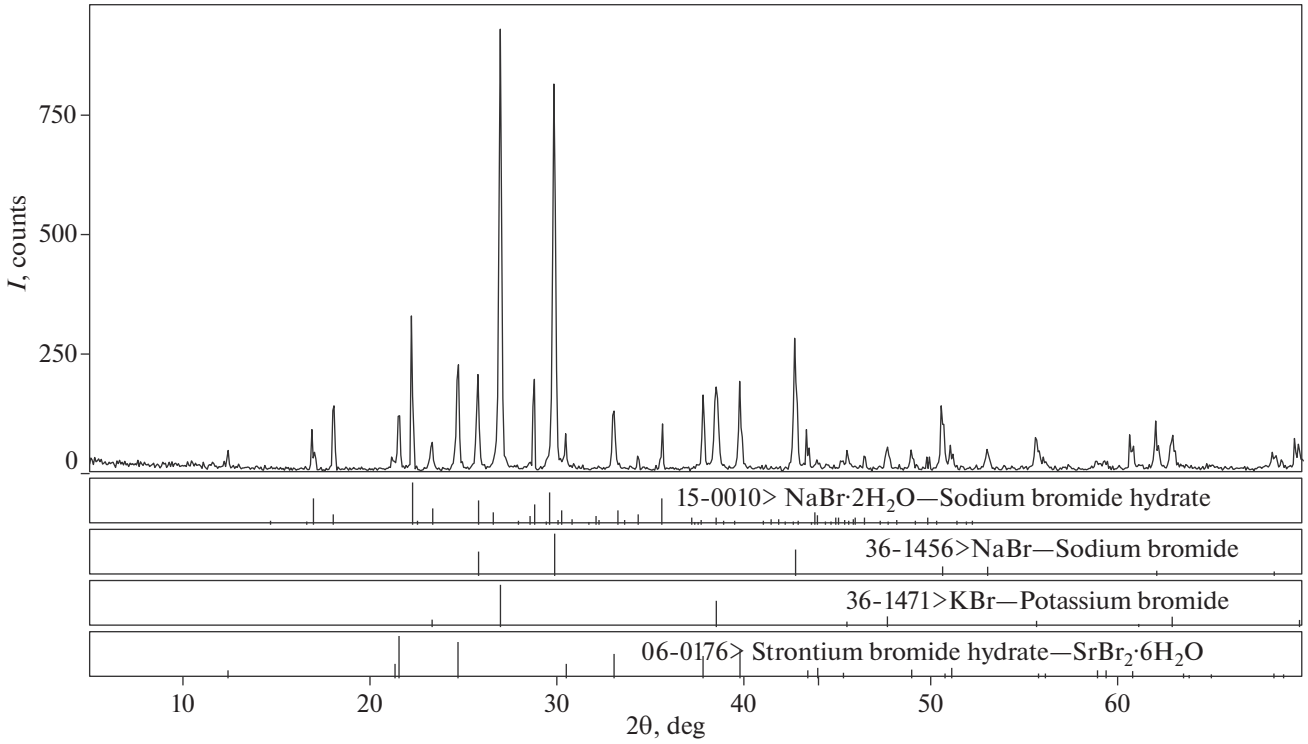

Fig. 6. X–ray powder diffraction photograph of equilibrium solid phases at invariant point E_3 (KBr + NaBr + $NaBr \cdot 2H_2O$ + $SrBr_2 \cdot 6H_2O$) in the quinary system LiBr–NaBr–KBr–$SrBr_2$–H_2O (saturated with KBr) at 308 K.

E_3 are shown in XRD diffraction patterns (Figs. 4–6). The experimental peak positions are basically consistent with the characteristic peaks of the standard card.

There are seven solubility curves AE_1, BE_3, CE_1, DE_2, FE_3, E_1E_2, and E_2E_3 in the dry basis phase diagram of the quinary system LiBr–NaBr–KBr–$SrBr_2$–H_2O, among them: (i) the univariant curve AE_1 is the solubility curve when $LiBr{\cdot}2H_2O$ + NaBr + KBr is co-saturated; (ii) the univariant curve BE_3 is the solubility curve when NaBr+$NaBr{\cdot}2H_2O$+KBr is co-saturated; (iii) the univariant curve CE_1 is the solubility curve when KBr + $LiBr{\cdot}2H_2O$ + $SrBr_2{\cdot}2H_2O$ is co-saturated; (iv) the univariant curve DE_2 is the solubility curve when $SrBr_2{\cdot}6H_2O$ + $SrBr_2{\cdot}2H_2O$ + KBr is co-saturated; (v) the univariant curve FE_3 is the solubility curve when $NaBr{\cdot}2H_2O$ + $SrBr_2{\cdot}6H_2O$ + KBr is co-saturated; (vi) the univariant curve E_1E_2 is the solubility curve when $SrBr_2{\cdot}2H_2O$ + NaBr + KBr is co-saturated; (vii) the univariant curve E_2E_3 is the solubility curve when $SrBr_2{\cdot}6H_2O$ + NaBr + KBr is co-saturated.

The seven solubility curves and three invariant points of the quinary system LiBr–NaBr–KBr–$SrBr_2$–H_2O dry basis diagram divide the phase diagram into five crystallization phase regions (in the presence of saturated solid phase KBr), they are $LiBr{\cdot}2H_2O$ crystallization area, NaBr crystallization area, $NaBr{\cdot}2H_2O$ crystallization area, $SrBr_2{\cdot}2H_2O$ crystallization area and $SrBr_2{\cdot}6H_2O$ crystallization area respectively. Among them, KBr has the smallest solubility and is easy to crystallize out, while $LiBr{\cdot}2H_2O$ has the largest solubility and the smallest crystallization area, which makes it difficult to separate out from a saturated solution. From the simplified dry basis phase diagram (Fig. 1) of the quinary system LiBr–NaBr–KBr–$SrBr_2$–H_2O (saturated with KBr) at 308 K, it can be found that the univariant curves AE_1, CE_1, and DE_2 are very short. While the curve $FE_3E_2E_1$ with the gradual addition of lithium bromide from the boundary point F has a very long trend, indicating that when the lithium bromide content is high, with the gradual addition of potassium bromide, sodium bromide or strontium bromide, the lithium bromide will no longer dissolve greatly. And it quickly stabilized and reached saturation. The content of each component does not change much. However, on the univariant curve $FE_3E_2E_1$ where lithium bromide is gradually added, from the data in Table 3 it can be seen that the contents of potassium bromide, sodium bromide and strontium bromide are gradually decreasing, the initial w(KBr) = 5.22%, w(NaBr) = 20.70%, $w(SrBr_2)$ = 31.67% reduced to w(KBr) = 2.10%, w(NaBr) = 0.60%, $w(SrBr_2)$ = 1.45%, while the content of lithium bromide gradually increased from zero to w(LiBr) = 60.57%, indicating that lithium bromide has a apparently salting-out effect on potassium bromide, sodium bromide and strontium bromide.

In this research, according to the Jänecke dry salt index J that calculated by mass fraction in Table 3, with $J(SrBr_2)$ as the abscissa and $J(H_2O)$ as the ordinate, the water content change of the quinary system at 308 K is plotted, as shown in Fig. 2. From the water content (Fig. 2), it is easy to find that on the isothermal solubility curve BE_3, the water content $J(H_2O)$ value in the saturated solution decreases with the increase of the $J(SrBr_2)$ value. On the univariant curve E_1F, the water content $J(H_2O)$ in the saturated solution initially increases with the increase of $J(SrBr_2)$, and then decreases with the increase of $J(SrBr_2)$, which is still related to the content of lithium bromide in two stages and its salting-out effect. While on the solubility curves AE_1, CE_1 and DE_2, the water content $J(H_2O)$ value of the saturated solution changes with the increase of the $J(SrBr_2)$ value not very obvious.

Besides, according to the Jänecke dry salt index J was calculated by mass fraction in Table 3, with $J(SrBr_2)$ as the abscissa and J(KBr) as the ordinate, the potassium bromide content of the quinary system LiBr–NaBr–KBr–$SrBr_2$–H_2O at 308 K is plotted as a function of the value of $J(SrBr_2)$, as shown in Fig. 3. From Fig. 3, it can be obviously found that the content of potassium bromide on the isothermal solubility curve BE_3 decreases with the increase of the $J(SrBr_2)$ value. On the isothermal solubility curves E_2E_3 and E_3F, the content of potassium bromide increases with the increase of the value of $J(SrBr_2)$. And the maximum content of potassium bromide is at point B (J = 10.18 g/100 g dry salt).

CONCLUSIONS

The phase equilibrium relationship of the quinary system LiBr–NaBr–KBr–$SrBr_2$–H_2O (when KBr is saturated) at 308 K was studied by the isothermal dissolution equilibrium method. The equilibrium liquid phase and solid phase in the system are studied by chemical analysis and X-ray powder crystal diffraction. The research results indicate that the quinary system neither generates solid solution nor double salt, so it is hydrate type. The dry basis phase diagram is composed of three invariant points, seven univariant curves, and five saturated solid phase crystallization regions. The five saturated solid-phase crystallization regions are $LiBr{\cdot}2H_2O$, NaBr, $NaBr{\cdot}2H_2O$, $SrBr_2{\cdot}2H_2O$, and $SrBr_2{\cdot}6H_2O$ respectively. Among them, KBr has the smallest solubility and is easiest to crystallize. $LiBr{\cdot}2H_2O$ has the smallest crystallization area, indicating that it has the largest solubility and is the most difficult to crystallize and separate from the mixed solution.

FUNDING

This project was supported by the National Natural Science Foundation of China (41873071) and Science and Technology Project of Sichuan Province (Key Research and Development Project 2021YFG0108), and the Natural Science Foundation of Qinghai Province (no. 2020-ZJ-970Q).

CONFLICT OF INTEREST

The authors declare that they have no conflicts of interest.

REFERENCES

1. J. B. Shao, Jilin Geology **32**, 1 (2013). https://doi.org/10.3969/j.issn.1001-2427.2013.03.001
2. J. B. Qin, D. M. Yu, and Y. B. Sun, Critical Rev. Analyt. Chem. **22**, 11 (2011). https://doi.org/10.3969/j.issn.1673-291X.2011.22.005
3. Y. T. Lin and S. X. Cao, Geology China **28**, 47 (2001). https://doi.org/CNKI:SUN:DIZI.0.2001-07-007
4. L. Ji, C. J. Liu, and N. J. Zheng, Mining Express **19**, 16 (2003). https://doi.org/CNKI:SUN:KYKB.0.2003-10-007
5. Z. Li, *Chengdu University of Technology Press: Chengdu, China* (2014). https://doi.org/CNKI:CDMD:2.1015.530148
6. Y. T. Lin and S. L. Chen, J. Salt Lake Res. **16**, 1 (2008). https://doi.org/10.1007/s00343-008-0023-6
7. Y. Zeng, F. J. Cao, and L. G. Li, J. Chem. Eng. Data **56**, 2569 (2011). https://doi.org/10.1021/je200091k
8. X. D. Yu, Y. Zeng, and H. X. Yao, J. Chem. Eng. Data **56**, 3384 (2011). https://doi.org/10.1021/je200360f
9. X. D. Yu, D. B. Jiang, and Q. Tan, J. Fluid Phase Equilib. **367**, 63 (2014). https://doi.org/10.1016/j.fluid.2014.01.037
10. X. D. Yu, Y. Zeng, and P. T. Mu, J. Fluid Phase Equilib. **387**, 88 (2015). https://doi.org/10.1002/aic.14825
11. X. D. Yu, Y. L. Luo, and L. T. Wu, J. Chem. Eng. Data **61**, 3311 (2016). https://doi.org/10.1021/acs.jced.6b00359
12. X. D. Yu, Y. Zeng, and S. S. Guo, J. Chem. Eng. Data **61**, 1246 (2016). https://doi.org/10.1021/je5008108
13. Q. H. Yin, Y. Zeng, and X. D. Yu, J. Chem. Eng. Data **58**, 2875 (2013). https://doi.org/10.1021/je400649r
14. J. J. Li, Y. Zeng, and X. D. Yu, J. Chem. Eng. Data **58**, 455 (2013). https://doi.org/10.1021/je301166y
15. Y. Zeng, H. A. Yin, and M. L. Tang, Chem. J. Chin. Univ. **24**, 968 (2003). https://doi.org/10.3321/j.issn:0251-0790.2003.06.005
16. Q. Tan, Y. Zeng, and P. T. Mu, J. Chem. Eng. Data **59**, 4173 (2014). https://doi.org/10.1021/je5008108
17. P. T. Mu, Q. Tan, and X. D. Yu, J. Chem. Eng. Data **60**, 574 (2015). https://doi.org/10.1021/je500700d
18. X. F. Guo, S. H. Sang, and H. Z. Zhang, Russ. J. Inorg. Chem. **66**, 916 (2021). https://doi.org/10.1134/S0036023621060097
19. X. P. Zhang, L. R. Zhao, and S. Y. Zhou, Russ. J. Inorg. Chem. **65**, 2062 (2020). https://doi.org/10.1134/S0036023620140089
20. S. Tursunbadalov, J. Inorg. Chem. **65**, 1213 (2020). https://doi.org/10.1134/S0036023620080197
21. S. H. Sang, X. Zhang, and J. J. Zhang, J. Chem. Eng. Data **57**, 907 (2012). https://doi.org/10.1021/je201138z
22. S. H. Sang and J. Peng, CALPHAD **34** 64-67(2010). https://doi.org/10.1016/j.calphad.2009.12.001
23. X. Zhang, S. H. Sang, and S. Y. Zhong, Russ. J. Phys. Chem. A **89**, 2322 (2015). https://doi.org/10.1134/S0036024415120316
24. K. J. Zhang, S. H. Sang, and T. Li, J. Chem. Eng. Data **58**, 115 (2013). https://doi.org/10.1021/je3009717
25. D. Wang, S. H. Sang, and X. X. Zeng, Petrochem. Ind. **40**, 285 (2011). https://doi.org/CNKI:SUN:SYHG.0.2011-03-011
26. S. H. Sang, X. Zhang, and J. J. Zhang, J. Chem. Eng. Data **57**, 907 (2011). https://doi.org/10.1021/je201138z
27. R. Z. Cui, S. H. Sang, and T. Li, CIESC J. **64**, 827 (2013). https://doi.org/10.3969/j.issn.0438-1157.2013.03.007
28. K. J. Zhang, S. H. Sang, and T. Li, J. Chem. Eng. Data **58**, 115 (2013). https://doi.org/10.1021/je3009717
29. Y. B. Weng, Y. F. Wang, and J. K. Wang, Chem. J. Chin. Univ. **21**, 695 (2007). https://doi.org/CNKI:SUN:GXHX.0.2007-04-027
30. D. Wang, S. H. Sang, and X. Zeng, J. Petrochem. Ind. **40**, 285 (2011). https://doi.org/10.3969/j.issn.1003-9015.2016.02.032
31. K. J. Zhang, S. H. Sang, and D. Wang, J. Salt Ind. Chem. Ind. **35**, 5 (2011). https://doi.org/10.3969/j.issn.1003-9015.2016.02.032
32. R. Z. Cui, S. H. Sang, and T. Li, Chem. Eng. J. **64**, 827 (2013). https://doi.org/10.3969/j.issn.0438-1157.2013.03.007
33. Y. X. Hu, S. H. Sang, and R. Z. Cui, Sci. Technol. Papers China **8**, 847 (2013). https://doi.org/10.3969/j.issn.2095-2783.2013.09.004
34. S. H. Sang, R. Z. Cui, and G. Liu, J. Chem. Eng. **30**, 472 (2016). https://doi.org/10.3969/j.issn.1003-9015.2016.02.032

35. C. Christov, CALPHAD **22**, 449 (1998). https://doi.org/10.1016/j.calphad.2003.08.001

36. B. Hu, P. S. Song, and Y. H. Li, CALPHAD **31**, 541 (2007). https://doi.org/10.1016/j.calphad.2007.03.002

37. X. X. Zeng, S. H. Sang, and D. Wang, Chem. Eng. **40**, 32 (2012). https://doi.org/10.1016/j.jct.2017.05.002

38. J. X. Hu, S. H. Sang, and Q. Z. Liu, J. Solut. Chem. **4**, 1963 (2015). https://doi.org/10.1007/s10953-015-0377-2

39. J. X. Hu, S. H. Sang, and Q. Z. Liu, J. Chem. Eng. Data **60**, 993 (2015). https://doi.org/10.1021/je500681m

40. J. X. Hu, S. H. Sang, and T. T. Zhang, J. Chem. Eng. Data **60**, 3087 (2015). https://doi.org/10.1021/acs.jced.5b00112

41. J. X. Hu, S. H. Sang, and M. F. Zhou, Fluid Phase Equilib. **392**, 127 (2015). https://doi.org/10.1016/j.fluid.2015.02.015

42. X. M. Jiang, F. Y. Li, and Z. L. Shi, J. Salt Chem. Ind. **41,** 25 (2012). https://doi.org/ir.isl.ac.cn/handle/363002/2702

43. *Institute of Qinghai Salt-Lake, Chinese Academy of Sciences* (Science Press, Beijing, 1988). https://doi.org/ISBN:7-03-000637-2

44. P. Manoravi and K. Shahi, Solid State Ionics **45**, 83 (1991). https://doi.org/10.1016/0167-2738(91)90106-L